Research Article | Vol. 26, No. 22 | 29 Oct 2018 | OPTICS EXPRESS 28349
Optics EXPRESS

Multi-vibration detection by probe pulses with ergodic SOPs in a POTDR system

XIANGCHUAN WANG,[1] JINTAO HU,[1] FENG WANG,[2] YINGQIONG YONG,[3] YIXIN ZHANG,[2] MIN XUE,[1] XUPING ZHANG,[2] AND SHILONG PAN[1,*]

[1]*The Key Laboratory of Radar Imaging and Microwave Photonics, Ministry of Education, Nanjing University of Aeronautics and Astronautics, Nanjing 210016, China*
[2]*The Institute of Optical Communication Engineering, College of Engineering and Applied Sciences, Nanjing University, Nanjing 210093, China*
[3]*R&D Center, China Academy of Launch Vehicle Technology, Beijing 100076, China*
**pans@nuaa.edu.cn*

Abstract: Polarization optical time domain reflectometers (POTDR) can detect vibration of fiber via the change of the state of polarization (SOP) of the Rayleigh backscattered light. For traditional POTDR systems, one key problem is the high misdiagnosis rate when multiple vibrations are simultaneously applied on the sensing fiber due to the random birefringence along the fiber. To solve this problem, we propose in this paper a novel implementation of the POTDR using probe pulses with ergodic SOPs. A series of vibration spectra along the fiber are obtained by sweeping the SOP of the probe pulse. The sum of these vibration spectra, which should be immune to the birefringence of the sensing fiber, is used to analyze the vibration information. Numerical simulation and experiments are carried out to analyze the performance of the proposed system when the input SOPs are traversed with uniform distribution and random distribution. Results show that the misdiagnosis rate of detecting multi-vibration with different frequencies is greatly reduced. In addition, detection of more-than-two vibrations with the same frequency based on POTDR is successfully performed for the first time to the best of our knowledge.

1. Introduction

Distributed optical fiber sensing has been extensively investigated in the past decades due to its superior performances over other conventional electrical sensors, e.g., long sensing distance, immunity to electromagnetic interference, and high sensitivity. Various technologies, such as optical time domain reflectometry (OTDR), Brillouin OTDR (BOTDR), Raman OTDR (ROTDR), phase OTDR (Φ-OTDR), and polarization OTDR (POTDR), have been proposed to achieve the information of temperature, stress, strain, vibration, electromagnetic field and so on [1–5], among which vibration is of great importance for perimeter security monitoring and aircraft structural health monitoring. Because the vibration along the optical fiber would change the SOP of the light traveling in it, the POTDR can realize vibration measurement by monitoring the change of the SOP of the Rayleigh backscattered light in fiber [6]. As compared with Φ-OTDR and BOTDR, which can also be applied for vibration measurement [7–10], POTDR features simple configuration and low cost. One key problem associated with traditional POTDRs, however, is its inefficiency to discriminate multiple vibrations with the same frequency. This is because the SOP of the light after the first vibration event would be modulated by the vibration frequency, and therefore it is hard to tell whether there exists a second vibration event if its frequency is the same as the first one. As a result, the previously-reported POTDRs were mostly used for monitoring vibrations with different frequencies [11,12]. For instance, Z. Zhang *et al.* proposed a POTDR based on frequency spectrum analyzing method [6] and H. Wu *et al.* demonstrated a POTDR using a 2-D image processing and statistical clustering method [11]. Both methods can detect multi-vibration

#340471 https://doi.org/10.1364/OE.26.028349
Journal © 2018 Received 24 Jul 2018; revised 23 Sep 2018; accepted 25 Sep 2018; published 16 Oct 2018

Optics EXPRESS

events with different frequencies, but cannot distinguish multiple vibrations when they have the same frequency. Y. Tong *et al.* achieved multi-event detection by employing a polarization maintaining fiber (PMF) as the distributed pressure sensor [13], but it is only suitable for static measurement. N. Linze *et al.* proposed another POTDR to detect multi-vibration events by using fiber Bragg grating (FBG) pairs [14], which is actually not distributed measurement. Recently, F. Wang *et al.* proposed a method for detecting two identical frequency vibrations by distinguishing the phase relationship of the two vibrations [15], which cannot be applied to detect more vibration events with the same frequency. In [16], we proposed a novel POTDR system using probe pulses with ergodic SOPs, which is potentially applied for multi-vibration event detection. But only some preliminary simulation results were reported, which was insufficient to understand the approach in-depth.

In this paper, a comprehensive theoretical and experimental investigation is performed on the POTDR system using probe pulses with ergodic SOPs which can distinguish the location and frequency information of multi-vibration events. The proposed system is effective even when vibrations have the same frequency. In Section 2, the proposed system is theoretically analyzed. Its feasibility to detect multi-vibration events is verified in Section 3 via numerical simulation, and the influence of the input SOP with uniform and random distribution is analyzed. Section 4 provides the experimental demonstration, and a conclusion is drawn in Section 5.

2. Principle and theoretical analysis

The schematic diagram of the proposed POTDR system using probe pulses with ergodic SOPs is shown in Fig. 1. A light wave from a laser diode (LD) is modulated by a probe pulse at a Mach-Zehner modulator (MZM). The SOP of the optical probe pulse is controlled using a polarization controller (PC). Then the optical probe pulse is injected into a length of sensing fiber which is disturbed by multiple vibrations. The SOP change of the Rayleigh backscattered light is transferred into intensity variation by a polarization beam splitter (PBS). Using a photodetector (PD) and an acquisition card (AC), the intensity variation is captured for obtaining the vibration information.

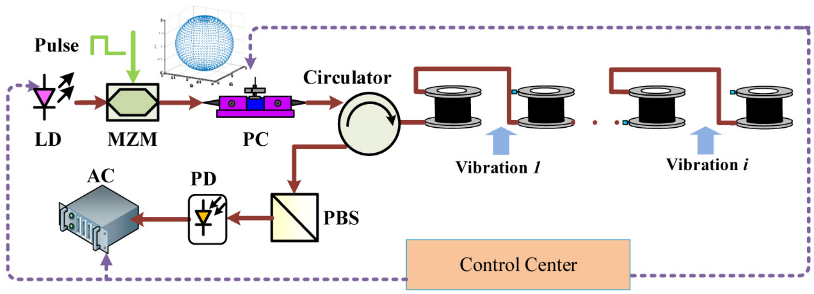

Fig. 1. The schematic diagram of the proposed POTDR system using probe pulses with ergodic SOPs. LD: laser diode; MZM: Mach-Zehner modulator; PC: polarization controller; PBS: polarization beam splitter; PD: photo-detector; AC: acquisition card.

To analyze the performance of the proposed system, a mathematical model based on the Muller matrix and waveplate model is set up. The evolution of the SOP of the light for forward propagation in the fiber can be denoted as [17]

$$\hat{S}_{\text{out}} = \vec{R}\hat{S}_{\text{in}} = R_z(\tau)R_y(\sigma)R_x(\gamma)R_y(-\sigma)R_z(-\tau)\hat{S}_{\text{in}} \quad (1)$$

where $\hat{S} = [S_0\ S_1\ S_2\ S_3]^T$ is the SOP of the light, γ depends on the linear birefringence, circular birefringence and rotation length of the sensing fiber, σ depends on the linear and circular

Optics EXPRESS

birefringences, and τ is the angle between the fast axis of the waveplate and the x-axis of the reference frame as in [17].

The matrix of the round-trip (forward propagation, scatters and back propagation down to the fiber head) can be written as [18]

$$\overleftarrow{R_B} = M\overrightarrow{R}^{T} M\overrightarrow{R} \tag{2}$$

where M is the mirror matrix.

As the birefringence axis of the fiber is not fixed and actually changed randomly, we subdivide the fiber into N birefringence segments with the uniform birefringence axis. In addition, the birefringence axis of each segment changes randomly to simulate the sensing fiber in practice. The waveplate length is $L_Z = L / N$ where L is the fiber length. We assume that the Muller matrices of the waveplates are R_1, R_2, ..., R_N, respectively. Then the SOP of the output light can be given by

$$\hat{S}_{out}(N \cdot L_Z) = H\overleftarrow{R_1}...\overleftarrow{R_i(\omega_i)}...\overleftarrow{R_j(\omega_j)}...\overleftarrow{R_q(\omega_q)}...\overleftarrow{R_N} \cdot \overrightarrow{R_N}...\overrightarrow{R_q(\omega_q)}...\overrightarrow{R_j(\omega_j)}...\overrightarrow{R_i(\omega_i)}...\overrightarrow{R_1}\hat{S}_{in} \tag{3}$$

where H is the Muller matrix of the PBS, $\overline{R_i(\omega_i)}$, $\overline{R_j(\omega_j)}$ and $\overline{R_q(\omega_q)}$ are the Muller matrices of the waveplates disturbed by vibrations respectively.

Due to Eq. (3) is too complicated to directly show the relationship between the SOP of the output light and the spectra of vibrations, an ideal cylindrical fiber with only random changed linear birefringence is assumed. The intrinsic circular-birefringence beat length is dozens of times higher than the linear-birefringence beat length, which means the intrinsic circular birefringence is very small in the sensing fiber [19]. Thus the circular birefringence of the sensing fiber can be neglected, which was also assumed in previous literatures [15,17]. On the other hand, the vibration is always induced by bending or stressing the fiber which would induce linear birefringence, not circular birefringence. Thus there are only the intrinsic linear birefringence and the linear birefringence induced by vibrations in the sensing fiber. Mathematically, the phase difference between the two orthogonal polarization axes induced by the ith vibration can be represented as [20]

$$\Delta\phi_i = k_i \cos(\omega_i t + \theta_i) \tag{4}$$

where k_i is the constant coefficient related to the amplitude of the vibration, the length of the disturbed fiber and the sensing fiber's intrinsic parameters such as fiber radius, photo-elastic coefficient, and refraction index, ω_i and θ_i are the frequency and phase of the vibration, respectively.

The intrinsic birefringence of the sensing fiber is simplified as linear birefringence. In addition, the birefringence induced by vibration is linear birefringence. The assumption that the birefringence induced by vibration is aligned with the intrinsic birefringence is also made in this article. In the remainder of the paper, the probe pulse duration is considered to be infinitely small to neglect the averaging over the spatial resolution. In addition, we also assume that the birefringence induced by the vibration remains unchanged during each probe pulse period.

The probe pulse travels forward to the position between the i-th vibration and $(i + 1)$-th vibration points. Then the pulse is scattered at the position and travels back to the fiber head. In this process, the SOP of the probe pulse would be changed by the birefringence induced by the front i vibrations and the intrinsic birefringence. After passing a PBS with the angle at 45° between x and y-axis, the intensity of the received scattered signal can be described as

$$P_i = \frac{1}{2}E_x^{\ 2} + \frac{1}{2}E_y^{\ 2} + Re(E_x E_y \cdot e^{j(\phi+\Delta\phi)}) \tag{5}$$

where ϕ is the initial phase difference between the two orthogonal axes, which depends on the SOP of the input probe light and the intrinsic birefringence of the sensing fiber. E_x and E_y are the amplitude of the input light at two birefringence axes, which can be described as:

$$E_x = E\cos(\delta) E_y = E\sin(\delta) \tag{6}$$

where the E is $(E_x^2+E_y^2)^{1/2}$, δ is the angle between the x-axis and the vector $E_x{*}e_x + E_y{*}e_y$ (e_x and e_y are the unit vectors along the x and y axis). The $\Delta\phi$ is the phase difference induced by the vibrations. As the SOP of the Rayleigh backscattered light would be disturbed by all vibrations before the scattering point, the total phase difference can be described as

$$\Delta\phi = 2\sum_{j=1}^{i}\Delta\phi_j \tag{7}$$

where j is the vibration number before the ith vibration.

Combined Eqs. (4)-(7), the following expression can be obtained by

$$\begin{aligned} P_i &= \frac{1}{2}E_x{}^2 + \frac{1}{2}E_y{}^2 + E_x E_y\cos(\phi+\Delta\phi) \\ &= \frac{1}{2}E_x{}^2 + \frac{1}{2}E_y{}^2 + E_x E_y[\cos(\phi)\cos(\Delta\phi) - \sin(\phi)\sin(\Delta\phi)] \\ &= \frac{1}{2}E_x{}^2 + \frac{1}{2}E_y{}^2 + E_x E_y[\cos(\phi)\cos(2\sum_{j=1}^{i}k_j\cos(\omega_j t+\theta_j)) - \sin(\phi)\sin(2\sum_{j=1}^{i}k_j\cos(\omega_j t+\theta_j))] \end{aligned} \tag{8}$$

The frequency spectrum of the intensity P_i mainly lies on the third component of Eq. (8). Based on the Jacobi-Anger expansion, Eq. (8) can be further expanded as the following expression when ignoring the DC component.

$$P_i \approx \left| E_x E_y\cos(\phi)\cdot\sum_{j=1}^{i}J_2(2k_j)\cos(2\omega_j t+2\theta_j) - E_x E_y\sin(\phi)\cdot\sum_{j=1}^{i}J_1(2k_j)\cos(\omega_j t+\theta_j)\right| \tag{9}$$

where J_1 and J_2 is the first and second order Bessel function.

For the cases that the vibration induced by bending the fiber, k is below 1 when the amplitude of vibration is below 2cm with 5cm bending radius [21]. In practice, the vibrations are usually much weaker, thus the amplitude of the second order Bessel function is much smaller than the first order Bessel function. Then Eq. (9) can be further simplified as

$$P_i \approx \left| E^2\cos(\delta)\sin(\delta)\sin(\phi)\cdot\sum_{j=1}^{i}J_1(2k_j)\right|\cdot\cos(\omega_j t+\theta_j) \tag{10}$$

Analyzing the frequency spectrum at each position as shown in Eq. (10), the position and frequency information of the vibrations along the sensing fiber can be obtained [6]. However, as it can be seen from Eq. (10), the amplitude of frequency not only depends on the constant coefficient k_j but also on the initial phase difference ϕ *and* δ. Since ϕ changes along the sensing fiber due to the random intrinsic birefringence, the amplitude of the frequency spectra fluctuates randomly along the fiber even though the fiber is disturbed by the same vibration.

For multiple vibrations with different frequencies using traditional POTDR, the amplitude of certain frequency components may be smaller than the threshold, which leads to a high misdiagnosis rate. For multiple vibrations with the same frequency, since the frequency components are the same at each position and the amplitude of each component is random along the fiber, it is nearly impossible to discriminate multiple vibrations from the frequency spectra of the signal for a traditional POTDR.

Optics EXPRESS

The system using probe pulses with ergodic SOPs is proposed to solve the above problems. The initial phase difference ϕ between the two orthogonal axes and the angle δ would be changed for each measurement. By adding up the amplitude of spectra generated from n ergodic SOPs, the spectrum amplitude of each vibration generated from the position after the ith vibration can be newly described as

$$A_{\text{sum}}(j)=\sum_{p=1}^{l}\sum_{q=1}^{m}\left|E^2\cos(\delta_p)\sin(\delta_p)\sin(\phi_q)\cdot J_1(2k_j)\right| \tag{11}$$

where $\phi_q\in[0,\pi]$, $\delta_p\in[0,\pi]$ are the initial phase difference between the two orthogonal axes and the angle between the input light and x-axis. Each ϕ, δ can represent a certain SOP.

If $n = l*m$ is large enough, Eq. (11) can be simplified as

$$\begin{aligned}A_{\text{sum}}(j)&=\int_0^{\pi}\sin(\phi_q)\mathrm{d}\phi_q*\sum_{p=1}^{l}\left|E^2\cos(\delta_p)\sin(\delta_p)\cdot J_1(2k_j)\right|\\&=2E^2\{\int_0^{\pi/2}\cos(\delta_p)\sin(\delta_p)\cdot J_1(2k_j)\mathrm{d}\delta_p+\int_{\pi/2}^{\pi}-\cos(\delta_p)\sin(\delta_p)\cdot J_1(2k_j)\mathrm{d}\delta_p\}\\&=2E^2\cdot J_1(2k_j)\end{aligned} \tag{12}$$

It can be seen from Eqs. (10)-(12) that the amplitude of the spectra depends only on the constant coefficient $J_1(2k_j)$ and the fixed initial phase of the vibration, which means the amplitude of the spectra only depends on the amplitude and number of the vibrations. Thus, for the detection of vibrations with different frequencies, the misdiagnosis rate induced by the amplitude random changing would be avoided. In addition, if vibrations along the sensing fiber are with the same frequency, the position information can also be obtained by analyzing the amplitude of the spectra because a newly vibration would change the amplitude of the spectra. In conclusion, using the proposed system, the misdiagnosis rate of detecting multiple vibrations with different frequencies could be reduced besides achieving multiple vibrations with same frequency detection.

3. Numerical simulation

In part 2, a mathematical model is proposed and verified by theoretical calculations, which can be used to directly show the relationship between the SOP of the output light and the spectra of vibrations. However, in practice, the angle between the fast axis of the waveplate and the reference axis would also randomly change along the sensing fiber, which makes the theoretical calculations more complicated. A numerical simulation considering the random change birefringence and birefringence axis based on Eq. (3) is used to analyze the performance of the proposed system. In the simulation, the following assumptions are taken:

1) $\tau_i\in\mu(0,\pi)$, where $\mu(0,\pi)$ is the random variable with a flat distribution between 0 and π.

2) There is no circular birefringence in the fiber.

3) The total length of the sensing fiber is 10 km while the length of each waveplate is 10 m.

4) The frequency resolution is 1 Hz while the frequency range is 500 Hz in the simulation.

3.1 Simultaneous vibrations with different frequencies

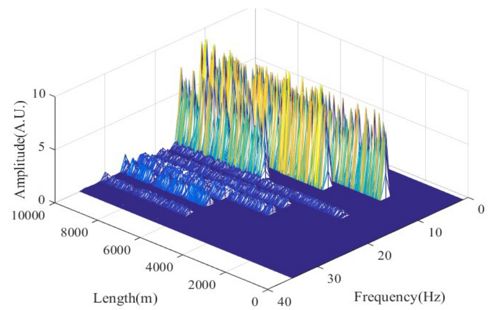

Fig. 2. The frequency spectra along the fiber generated from one SOP.

The fiber is assumed to be disturbed by three vibrations with different frequencies of 8 Hz, 11 Hz, and 15 Hz at 2 km, 4 km and 6 km simultaneously. For a probe pulse with a certain SOP, the time domain signal along the sensing fiber is obtained for 1000 times. Then the spectra along the sensing fiber can be obtained using FFT shown in Fig. 2 which contains the frequency information along the sensing fiber. The frequency spectra contain 8 Hz component after 2 km, 8 Hz, and 11 Hz components after 4 km and 8 Hz, 11 Hz and 15 Hz components after 6 km. The 16 Hz, 22 Hz, and 30 Hz are the double frequency components of the vibration frequencies which are caused by the high amplitude of the vibration as shown in Eq. (9). The 19 Hz is the second-order term of the 8 Hz and 11 Hz.

However, as shown in Fig. 3, in the detailed spectra within one beat length, the amplitudes are variable at different positions. This is because the amplitude depends on the SOP of the probe light at the position. As the SOP is random changed along the sensing fiber due to the random birefringence, the amplitude of spectra would also change randomly. Although all frequency components are contained in the spectra, some components may too small to be detected. For example, the vibration with a frequency of 11 Hz in Fig. 3(b), and the vibration with frequencies of 8 Hz and 15 Hz in Fig. 3(d) would be omitted by just analyzing the amplitude of the spectra at a certain position. Thus, it would cause a high false negative rate.

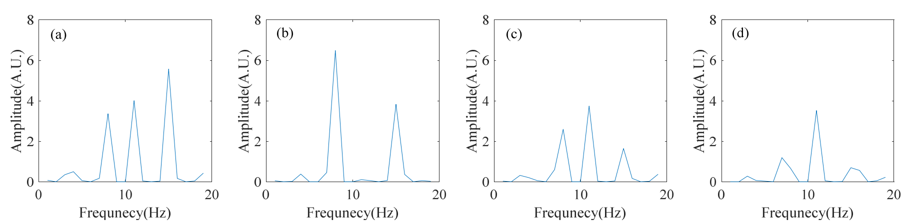

Fig. 3. The frequency spectra along the fiber generated from one SOP within one beat length: (a) at 6000 m; (b) at 6010 m; (c) at 6020 m; (d) at 6030 m respectively.

To solve the above problem, the input SOPs are changed to get different spectra. The SOPs distribution of the probe pulse in the proposed scanning method is randomly covered the Poincare sphere. There are 4225 points on the Poincare sphere, and each point corresponds one certain SOP of the probe pulse. Therefore, a series of vibration spectra along the fiber are obtained. Then by adding up these spectra, the new spectra are used to distinguish the frequency and location information of the vibrations.

Optics EXPRESS

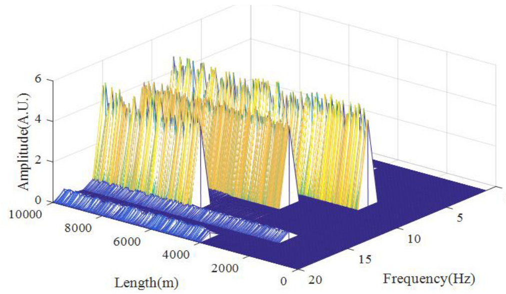

Fig. 4. The frequency spectra along the fiber generated from ergodic SOPs.

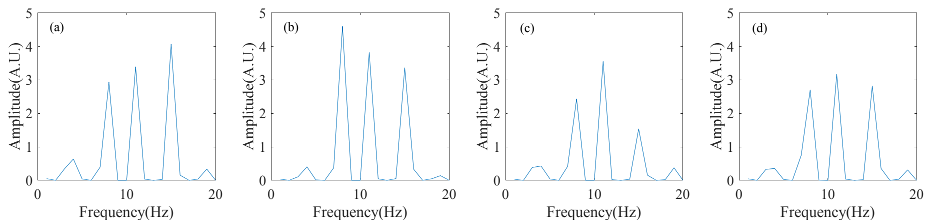

Fig. 5. The frequency spectra along the fiber generated from ergodic SOPs within one beat length: (a) at 6000 m; (b) at 6010 m; (c) at 6020 m; (d) at 6030 m respectively.

Figure. 4 shows the added-up spectra along the fiber generated from ergodic SOPs. The result of ergodic SOPs has a better flat amplitude response compared to the result of single SOP. And the amplitude fluctuations at the frequency of 15 Hz, 11 Hz, and 8 Hz are obviously reduced. As shown in Fig. 5, compared with the corresponding figure in Fig. 3, the amplitude of the concern frequencies around 6 km are much better flat, which is only related to the vibration amplitude of the event. The effect of the probe light SOP and birefringence on the amplitude of the spectra are greatly restrained. The amplitude of each frequency component would not change with the fiber length. Consequently, the misdiagnosis rate is greatly reduced.

Figure. 6 shows the amplitude of the 11 Hz component along the fiber with single SOP and with ergodic SOPs. As the 11 Hz vibration is induced at 4 km, the 11 Hz component of spectra only appears after 4 km. The standard deviation of the amplitude of 11 Hz component with a single SOP is about 2.27 while the result is 0.98 with ergodic SOPs, which means the flatness is improved by 3.6 dB.

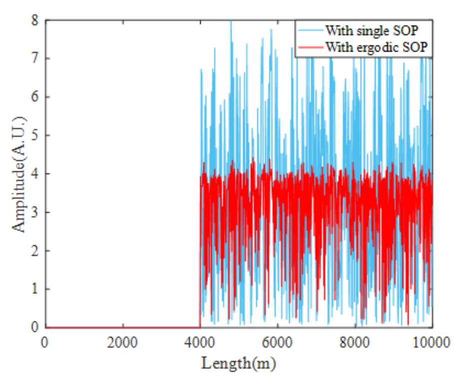

Fig. 6. The amplitude of 11 Hz component along the fiber with single SOP or with ergodic SOPs.

As the number of the ergodic SOPs would influence the accuracy of the results, we change the value of n to obtain different results. The standard deviation of the amplitude of 11 Hz component with different values of n is shown in Fig. 7. As it seen, when n is below 1470, the standard deviation would reduce monotonously from 2.27 to 0.89. When n is larger than 1470, the standard deviation of the amplitude of 11 Hz component would be around 1. Therefore, the largest improvement of the flatness of the proposed system is about 4.1 dB.

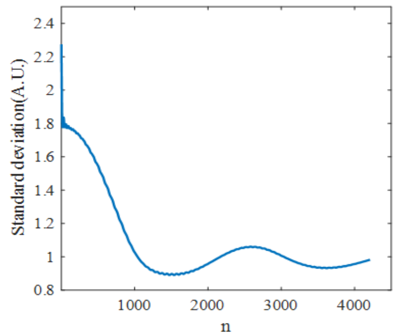

Fig. 7. The standard deviation of the amplitude of 11 Hz component with different value of *n*.

3.2 Simultaneous events with the same vibration frequencies

In section 3.1, we demonstrate the feasibility of detecting multiple simultaneous vibrations with different frequencies, which should be sufficient for some applications. However, in some situations in practice, it might happen that two or more simultaneous events have exactly the same vibration frequency. The method, adding up spectra generated from ergodic SOPs, is proposed to distinguish the locations of multi-vibrations with the same frequency in POTDR system which is hard to be achieved in the traditional POTDR system.

For the traditional POTDR system, when the vibrations along the fiber are with the same frequency, actually we set three vibrations with 11 Hz at 2 km, 4 km, 6 km respectively in the simulation, the result is shown in Fig. 8. From Fig. 8, we can see that the spectra before the first vibration have no frequency component. After the first perturbation at 2 km, the amplitudes of the vibration spectra fluctuate along the fiber irregularly, and the standard deviation of the peak in Fig. 8 is about 2.9. Such high standard deviation makes that we can only obtain the first vibration's frequency and location while the second and third vibrations are hard to be distinguished.

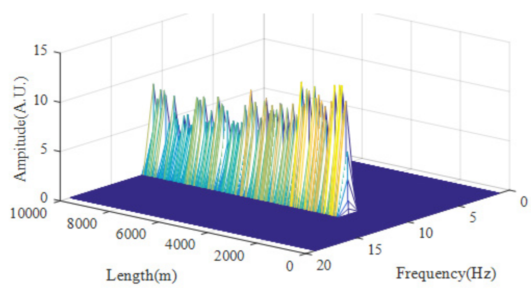

Fig. 8. The frequency spectra along the fiber generated from one SOP.

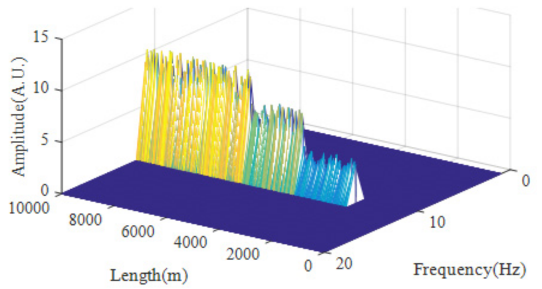

Fig. 9. The frequency spectra along the fiber generated from ergodic SOPs with uniform distribution.

In the next, we proposed two ways of the scanning the SOP of the probe pulse to curb the amplitude's irregular fluctuation. Firstly, the SOP of the probe light is changed to uniformly cover the Poincare sphere. A series of vibration spectra along the fiber are obtained. The frequency spectrum from the sum of these vibration spectra is shown in Fig. 9. In Fig. 9, we can see the irregular fluctuation is effectively controlled compared to the spectra obtained with only one fixed SOP. Each step along the curve is flatter than the result of the single SOP in Fig. 6, and standard deviation of the peak in Fig. 9 is reduced for 3.9 dB from 2.9 to 1.16 after divided by 4225 times because of the superposition. As the amplitude of the latter vibration's spectrum is dependent on the previous vibrations, there would be a difference among the amplitudes of multi-vibration spectra. As shown in Fig. 9, except the appearance of the frequency component (11 Hz) at the first vibration (2 km), there are also two amplitude changes at 4 km and 6 km respectively, which correspond to the second and third vibrations. Therefore, the method of scanning the SOP of the probe pulse can be proved to detect the multi-vibrations with the same frequency along the fiber.

Secondly, we set the SOPs of the probe pulse as a random distribution which is much easier to be achieved using a polarization scrambler. In this method, we obtain the frequency spectra under 4225 SOPs which are randomly changed. The adding up frequency spectra at each position is shown in Fig. 10. The result shows that there are two more obvious amplitude mutations at 4 km and 6 km, corresponding with the second and third vibrations respectively. And the standard deviation of the peak in Fig. 10 is reduced by 3.4 dB from 2.9 to 1.3 after being divided by 4,225 times because of the superposition. Therefore, the multi-vibration with same frequency can also be detected by our proposed system using random distribution SOPs.

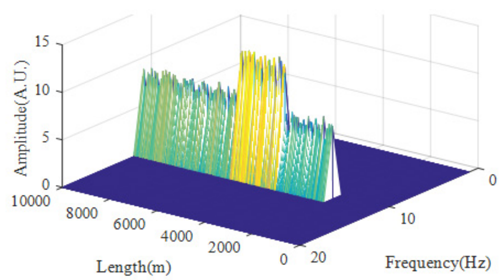

Fig. 10. The frequency spectra along the fiber generated from ergodic SOPs with random distribution.

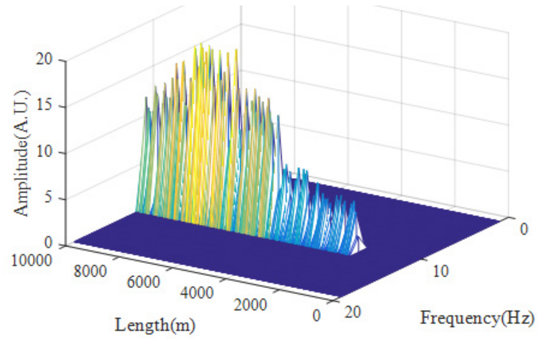

Fig. 11. The frequency spectra generated from one fixed SOP when there are five vibrations along the sensing fiber.

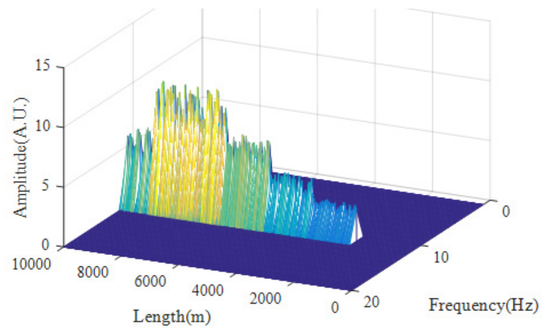

Fig. 12. The frequency spectra generated from ergodic SOPs with random distribution when there are five vibrations along the sensing fiber.

To verify the feasibility of the method in multi-events detecting, we set five simultaneous vibrations with the same vibration frequencies at 2 km, 4 km, 6 km, 7 km and 9 km. With the spectra obtained by one fixed SOP, only the first vibration at 2 km is distinguished while the other vibrations are missed as shown in Fig. 11. In compare, 4225 randomly changed SOPs are used to obtain the add-up spectra, shown in Fig. 12. The five vibrations can be obviously distinguished by determining the amplitude changes.

4. Experimental results and discussion

A proof-of-concept experiment is carried out as shown in Fig. 1. A light from a laser source with 0.1 nm bandwidth and 17 dBm peak power is sent to an MZM with 40 dB extinction ratio to generate a 100 ns probe pulse with a period of 100 μs. The SOP of the probe pulse changed by the PC is then sent into a 2 km sensing fiber which is disturbed by three vibrations at 0.5 km, 1 km, and 1.5 km, respectively. The Rayleigh backscattered light passing through a circulator is polarized by PBS to monitor the SOP change of the back Rayleigh scattering along the sensing fiber. After a PD with 20 MHz bandwidth and 10^6 gain, the electrical sensing signal is captured by a data AC with 100 MSa/s sampling rate and 16-bit sampling number for further processing.

Optics EXPRESS

4.1 Multiple vibrations with different frequencies

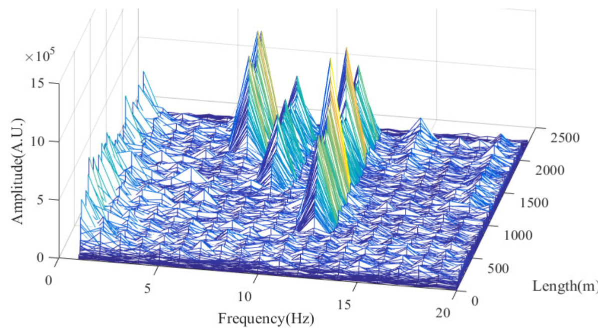

Fig. 13. The spectra along the fiber with one fixed SOP when three vibrations with different frequencies are induced.

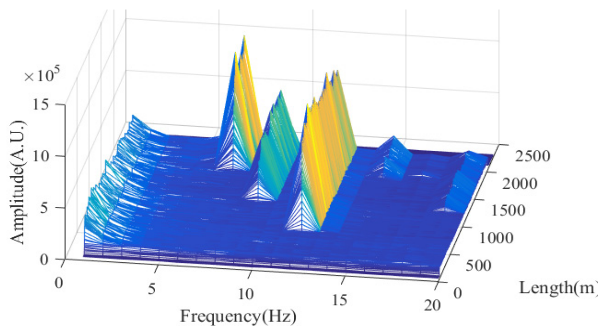

Fig. 14. The spectra along the fiber with ergodic SOPs when three vibrations with different frequencies are induced.

To verify the feasibility of reducing the misdiagnosis rate of the proposed system in detecting multi-vibration with different frequencies, three vibrations with frequencies of 7 Hz, 9 Hz and 12 Hz are induced at 0.5 km, 1 km, and 1.5 km respectively using a mechanical vibration device. Firstly, the SOP of the probe pulse is fixed and the sensing signal is captured by 1 second. Thus the frequency resolution of the system is 1 Hz. The spectra along the sensing fiber are shown in Fig. 13. The spectra contain 12 Hz component after 1 km, 9 Hz after 1.5 km and 7 Hz after 2 km. It can be seen that the fluctuation of the certain useful frequency component is large along the sensing fiber, which is disadvantaged to the determination of vibrations' amplitude and position information. Secondly, the SOP of the probe pulse is changed randomly for 100 times using PC. For each SOP, the spectra along the fiber are obtained. Then the 100 spectra are added up and averaged as shown in Fig. 14. The signal to noise ratio is improved for about 5 dB. Moreover, the amplitude fluctuation of the concerned components is much flatter which is benefited for the determination of the vibrations as analyzed in the numerical simulation.

The detailed spectra within one beat length (about 40 m for single-mode fiber) around 1.6 km are shown in Fig. 15. There are large differences among the amplitudes of the three vibration components at different positions when using single SOP, which make it hard to give the threshold, and high misdiagnosis rate would be induced. For example, the 9 Hz and 12 Hz in Fig. 15(a) and 9 Hz in Figs. 15(b)-15(d) would be missed. When the ergodic SOPs are used, the amplitudes of the spectra are much higher and more stable. For example, the 7 Hz, 9 Hz and 12 Hz components are more obvious making it much easier to distinguish vibrations at each position.

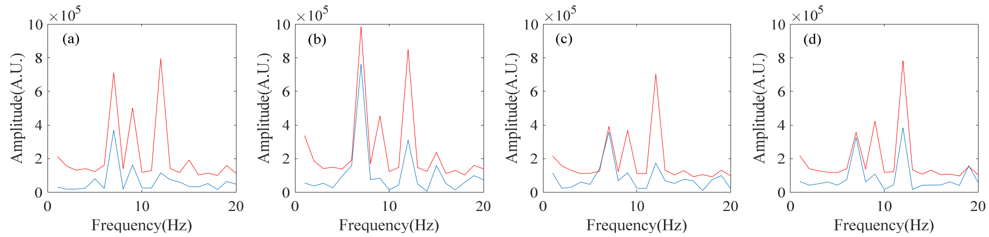

Fig. 15. The frequency spectra along the fiber generated from single fixed SOP and ergodic SOPs: (a) at 1600 m; (b) at 1610 m; (c) at 1620 m; (d) at 1630 m, respectively.

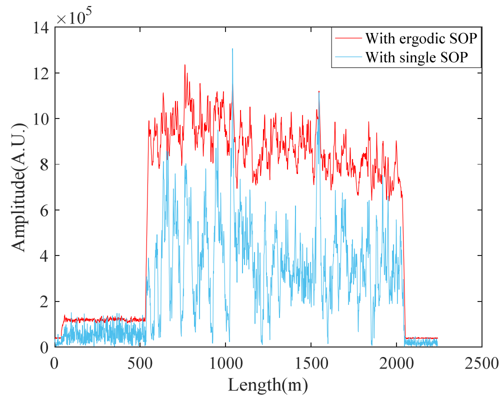

Fig. 16. The amplitude of 12 Hz component along the fiber with single SOP or with ergodic SOPs.

The 12 Hz component along the fiber obtained by single SOP and ergodic SOPs are shown in Fig. 16. Due to the SOP change along the fiber when one single SOP is used, the amplitude of the component is fluctuating along the fiber. The low amplitude would induce erroneous judgment. When the ergodic SOPs are used, the amplitude fluctuation is much smaller. As shown in Fig. 16, the amplitude standard deviation with ergodic SOPs is reduced by about 2.3 dB from 1.9×10^5 to 1.1×10^5. Then the influence of the random change birefringence on the amplitude of vibration spectrum is weakened, which reduces the misdiagnosis rate of POTDR on detecting multi-vibration with different frequencies, consequently. Compared with the standard deviation of the simulation, which is reduced by about 3.6 dB, the experimental result is a little bit small, which may be caused by two reasons. The first one is the number of the ergodic SOPs is 100 in the experiment while the number of the ergodic SOPs is 4225 in the simulation, which would the experimental results. The second on is that the phase of the vibration would also affect the results of the proposed system as shown in Eq. (9). As the phase of vibration in the simulation is assumed unchanged with different SOPs while the phase of the vibration would change during the SOPs changing period, the experimental results would be worse than the simulation results.

4.2 Multiple vibrations with the same frequencies

To verify the feasibility of detecting multi-vibration with the same frequency, three vibrations with a frequency of 12 Hz are induced at 0.5 km, 1 km, and 1.5 km, respectively. The spectra obtained using the probe pulse with a fixed SOP is shown in Fig. 17. There is only 12 Hz component in the spectra after 0.5 km. Due to the large fluctuation of the 12 Hz component, only the first vibration can be certified by analyzing the spectra. The second and third vibrations at 1 km and 1.5 km are missed.

Then the SOP of the probe pulse is changed randomly for 100 times using PC. The adding up spectra along the sensing fiber are shown in Fig. 18. The fluctuation of the 12 Hz component

Optics EXPRESS

between two adjacent vibrations is greatly reduced, which make it obvious to justify the amplitude change induced by the newly vibration. Thus, multi-vibration detection with the same frequency is achieved by the proposed system.

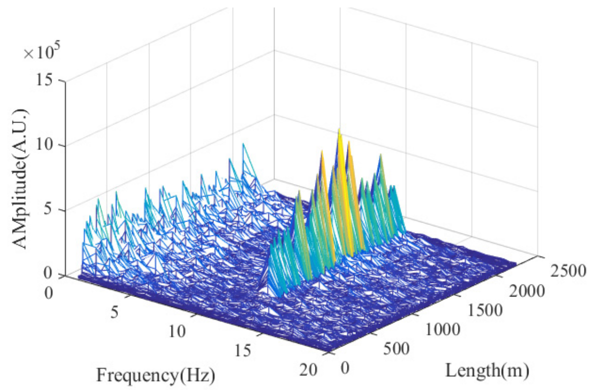

Fig. 17. The spectra obtained with one single SOP along the sensing fiber when the fiber is disturbed by three vibrations with the same frequency of 12 Hz.

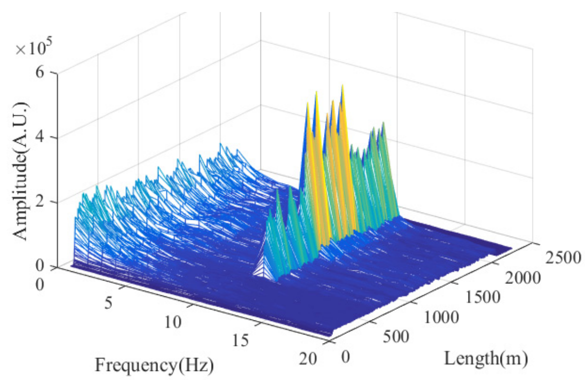

Fig. 18. The spectra obtained with ergodic SOPs along the sensing fiber when the fiber is disturbed by three vibrations with the same frequency of 12 Hz.

It is necessary to note here, only vibrations with low frequencies around 10 Hz are used in this proof-of-concept experiment due to the limitation of the mechanical vibration device's frequency range. Because the final spectra for multi-vibrations detection are obtained by adding several spectra with different SOPs. For each spectrum with certain SOP, the frequency range depends on the pulse period. The summation is achieved in the frequency domain, it would not be affected by the time *t*. Thus, the frequency range of the proposed system is still only related to the pulse period which should be large enough to make sure that only one pulse in the sensing fiber at a certain time. However, in order to achieve the best results, it should be required that the vibration should be persisted during the period of ergodic SOPs, which means the response time of the proposed system would be increased for *n* times compared to the traditional POTDR system.

5. Summary

In this article, a distributed fiber sensing system based on the POTDR technique with ergodic SOPs for multi-vibration detection is proposed and demonstrated. For the detection of multiple vibrations with different frequencies in the traditional POTDR system, the amplitude variation of each frequency component along the sensing fiber induced by the randomly changed birefringence in the fiber can be greatly reduced. Then the accuracy of distinguishing multi-vibration with different frequencies is improved. In addition, the feasibility of the detection of multiple vibrations with the same frequency which cannot be detected using the traditional POTDR system is also analyzed and demonstrated with numerical simulation and experiment. In summary, multi-vibrations with different frequencies or the same frequency are successfully detected using the proposed system which would greatly promote the development of POTDR system and multi-vibration detection.

6. Funding

National Natural Science Foundation of China (61605077, 61527820); Fundamental Research Funds for the Central Universities (NC2018005).

References

1. Q. Sun, F. Ai, D. Liu, J. Cheng, H. Luo, K. Peng, Y. Luo, Z. Yan, and P. P. Shum, "M-OTDR sensing system based on 3D encoded microstructures," Sci. Rep. **7**(1), 41137 (2017).
2. Q. Zhao, L. Xia, C. Wan, J. Hu, T. Jia, M. Gu, L. Zhang, L. Kang, J. Chen, X. Zhang, and P. Wu, "Long-haul and high-resolution optical time domain reflectometry using superconducting nanowire single-photon detectors," Sci. Rep. **5**(1), 10441 (2015).
3. Y. Mizuno, N. Hayashi, H. Fukuda, K. Y. Song, and K. Nakamura, "Ultrahigh-speed distributed Brillouin reflectometry," Light Sci. Appl. **5**(12), e16184 (2016).
4. F. Peng, H. Wu, X. H. Jia, Y. J. Rao, Z. N. Wang, and Z. P. Peng, "Ultra-long high-sensitivity Φ-OTDR for high spatial resolution intrusion detection of pipelines," Opt. Express **22**(11), 13804–13810 (2014).
5. A. J. Rogers, "Polarization-optical time domain reflectometry: a technique for the measurement of field distributions," Appl. Opt. **20**(6), 1060–1074 (1981).
6. Z. Zhang and X. Bao, "Distributed optical fiber vibration sensor based on spectrum analysis of Polarization-OTDR system," Opt. Express **16**(14), 10240–10247 (2008).
7. J. C. Juarez and H. F. Taylor, "Polarization discrimination in a phase-sensitive optical time-domain reflectometer intrusion-sensor system," Opt. Lett. **30**(24), 3284–3286 (2005).
8. Y. Lu, T. Zhu, L. Chen, and X. Bao, "Distributed Vibration Sensor Based on Coherent Detection of Phase-OTDR," J. Lightwave Technol. **28**(22), 3243–3249 (2010).
9. F. Peng, N. Duan, Y. J. Rao, and J. Li, "Real-Time Position and Speed Monitoring of Trains Using Phase-Sensitive OTDR," IEEE Photonics Technol. Lett. **26**(20), 2055–2057 (2014).
10. C. Jin, N. Guo, Y. Feng, L. Wang, H. Liang, J. Li, Z. Li, C. Yu, and C. Lu, "Scanning-free BOTDA based on ultra-fine digital optical frequency comb," Opt. Express **23**(4), 5277–5284 (2015).
11. H. Wu, J. Liu, L. Lu, X. Sun, D. Atubga, and Y. Rao, "Multi-Point Disturbance Detection and High-Precision Positioning of Polarization-Sensitive Optical Time-Domain Reflectometry," J. Lightwave Technol. **34**(23), 5371–5377 (2016).
12. X. Wang, C. Wang, M. Tang, S. Fu, and P. Shum, "Multiplexed polarization OTDR system with high DOP and ability of multi-event detection," Appl. Opt. **56**(13), 3709–3713 (2017).
13. Y. Tong, H. Dong, Y. Wang, W. Sun, X. Wang, J. Bai, H. Yuan, N. Zhu, and J. Liu, "Distributed incomplete polarization-OTDR based on polarization maintaining fiber for multi-event detection," Opt. Commun. **357**, 41–44 (2015).
14. N. Linze, P. Tihon, O. Verlinden, P. Mégret, and M. Wuilpart, "Development of a multi-point polarization-based vibration sensor," Opt. Express **21**(5), 5606–5624 (2013).
15. F. Wang, Y. Pan, M. Zhang, C. Cao, and X. Zhang, "Detection of two identical frequency vibrations by phase discrimination in polarization-OTDR," Opt. Commun. **389**, 247–252 (2017).
16. J. Hu, X. Wang, and S. Pan, "Application of the probe pulse with ergodic SOPs in detecting multi-vibrations using POTDR," Proc. SPIE **10618**, 1061805 (2018).
17. F. Corsi, A. Galtarossa, and L. Palmieri, "Polarization mode dispersion characterization of single-mode optical fiber using backscattering technique," J. Lightwave Technol. **16**(10), 1832–1843 (1998).
18. F. Corsi, A. Galtarossa, and L. Palmieri, "Beat length characterization based on backscattering analysis in randomly perturbed single-mode fibers," J. Lightwave Technol. **17**(7), 1172–1178 (1999).
19. A. Galtarossa and L. Palmieri, "Measure of twist-induced circular birefringence in long single-mode fibers: Theory and experiments," J. Lightwave Technol. **20**(7), 1149–1159 (2002).
20. X. Wang, X. Zhang, F. Wang, M. Chen, and C. Li, "Application of frequency spectrum analysis in measuring multi-vibrations by using POTDR," Proc. SPIE **8198**, 819808 (2011).
21. R. Ulrich, S. C. Rashleigh, and W. Eickhoff, "Bending-induced birefringence in single-mode fibers," Opt. Lett. **5**(6), 273–275 (1980).